Impact of urban pollution on freshwater biofilms: Oxidative stress, photosynthesis and lipid responses

Caroline Roux, Cassandre Madru, Débora Millan-Navarro, Gwilherm Jan, Nicolas Mazzella, Aurélie Moreira, Jacky Vedrenne, Laure Carassou, Soizic Morin

Journal of Hazardous Materials 472 (2024) 134523

Contents lists available at ScienceDirect

Journal of Hazardous Materials

journal homepage: www.elsevier.com/locate/jhazmat

Impact of urban pollution on freshwater biofilms: Oxidative stress, photosynthesis and lipid responses

Caroline Roux [a,*], Cassandre Madru [a], Débora Millan Navarro [a], Gwilherm Jan [a], Nicolas Mazzella [a,b], Aurélie Moreira [a,b], Jacky Vedrenne [a], Laure Carassou [a], Soizic Morin [a]

[a] INRAE, UR EABX, 50 avenue de Verdun, 33612 Cestas cedex, France
[b] Bordeaux Metabolome, MetaboHUB, PHENOME-EMPHASIS, Villenave d'Ornon 33140, France

HIGHLIGHTS

- Light pollution affects photosynthetic parameters.
- DDBAC generates oxidative stress on fatty acids with an increase of oxylipins.
- Oxylipins can be a biomarker of biocide exposure in aquatic environment.

GRAPHICAL ABSTRACT

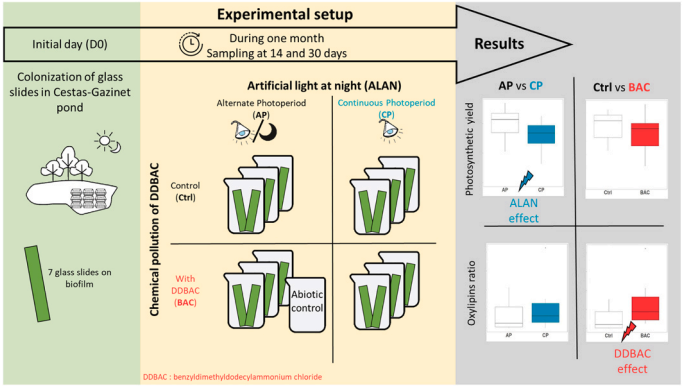

ARTICLE INFO

Keywords:
Artificial light at night (ALAN)
Chemical pollution
Dodecylbenzyldimethylammonium chloride (DDBAC)
Fatty acids
Oxylipins
Aquatic ecosystems

ABSTRACT

Urban ecosystems are subjected to multiple anthropogenic stresses, which impact aquatic communities. Artificial light at night (ALAN) for instance can significantly alter the composition of algal communities as well as the photosynthetic cycles of autotrophic organisms, possibly leading to cellular oxidative stress. The combined effects of ALAN and chemical contamination could increase oxidative impacts in aquatic primary producers, although such combined effects remain insufficiently explored. To address this knowledge gap, a one-month experimental approach was implemented under controlled conditions to elucidate effects of ALAN and dodecylbenzyldimethylammonium chloride (DDBAC) on aquatic biofilms. DDBAC is a biocide commonly used in virucidal products, and is found in urban aquatic ecosystems. The bioaccumulation of DDBAC in biofilms exposed or not to ALAN was analyzed. The responses of taxonomic composition, photosynthetic activity, and fatty acid composition of biofilms were examined. The results indicate that ALAN negatively affects photosynthetic yield and chlorophyll production of biofilms. Additionally, exposure to DDBAC at environmental concentrations induces lipid peroxidation, with an increase of oxylipins. This experimental study provides first insights on the consequences of ALAN and DDBAC for aquatic ecosystems. It also opens avenues for the identification of new biomarkers that could be used to monitor urban pollution impacts in natural environments.

* Corresponding author.
E-mail address: caroline.roux@inrae.fr (C. Roux).

https://doi.org/10.1016/j.jhazmat.2024.134523
Received 16 February 2024; Received in revised form 30 April 2024; Accepted 1 May 2024
Available online 6 May 2024

1. Introduction

Urban aquatic ecosystems are subjected to a multitude of anthropogenic stresses leading to vulnerable biological communities. Among physical urban stressors, Artificial Light at Night (ALAN) is widespread in all urban environments in the world, with more than 80% of the world human population (and more than 99% in North America and Europe) living under light-polluted skies [21]. Light is defined by multiple dimensions including its intensity (in W m^{-2}), temperature (in kelvin), wavelength (in nm) and photoperiod [7]. The occurrence of ALAN in cities can change the quantity and quality of light at night as compared to natural conditions [75]: a continuous illumination often occurs over time, changing natural photoperiods, and the intensity, temperature and spectra of light exposure at night is modified by the use of LEDs (Light-Emitting Diodes; [99]). Human circadian rhythmicity was also shown to be affected by ALAN [77]. ALAN does not only affect the terrestrial world, but can also alter aquatic ecosystems [28]. After penetration below the water surface, diffraction and reflection, the residual light intensity and wavelengths vary according to the physical and biological characteristics of the water (salinity, density, suspended matter, including biological particles, e.g. plankton). Light effects in the natural environment also depend on other environmental factors such as lunar cycles, cloud cover, the influence of shading, etc. [43]. Some wavelengths do penetrate below the surface down to 40 m depth depending on water clarity [73]. As a result, 3.1% of the world's marine economic zones are impacted at 10 m depth, and the influence of artificial light is still observable at 20 m [73]. Among reported biological effects, ALAN can lead to changes in the composition of aquatic algal communities [32], disruption of photosynthetic cycles [49], or alteration of species interactions [60].

Among chemical urban pressures, quaternary ammonium compounds (QACs) are reported in aquatic environments worldwide [96]. QACs are found in the most commonly used disinfectants for their cationic detergents properties [31]. The use of QACs has considerably increased since the ban of triclosan in 2016 [55], because of their high efficiency, low ecotoxicity and broad spectrum action [59,89]. QACs are composed of a central nitrogen atom with four attached groups (e.g., nitrogen atoms, branching of the carbon chain, the presence of aromatic and methyl groups). The negatively charged anion portion like chlorine or bromine is linked to nitrogen to form the QAC salt [31]. Among QACs, benzalkonium chloride-based substances (BAC) have an aromatic group, two groups of methyl and an alkyl chain of length from C8 to C18 [6]. Methyl group lengths of C12 to C16 usually show the greatest antimicrobial activity [31]. Therefore, BAC are used to clean bactericide residues in food products [5] and as a preservative in diversified commercial personal care products [76]. Europe established thresholds for BAC concentrations which are limited to 0.3% in cosmetics and 0.2% in mouthwashes by SCCP (Scientific Committee on Consumer Products; [20]). BAC biocides were also recommended by the US EPA (Environmental Protection Agency) for disinfecting surfaces against SARS-CoV-2 [58,84,97]. As a result of this increased use, several studies highlighted potential antibiotic resistance to BAC products in bacteria [34,47,62,92], with an associated production of Extracellular Polymeric Substances (EPS). The ubiquitous and frequent use of BAC can thus generate selective environments, favoring resistant microorganisms [45,56]. Furthermore, BAC compounds were shown to decrease photosynthetic efficiency and growth in green algae [18,29,98] or to enhance the production of reactive oxygen species (ROS) in diatoms [17] and cyanobacteria [95]. Among the different forms of BAC, dodecylbenzyldimethylammonium chloride (DDBAC) is the most occurrent in wastewater from sewage treatment plants [14] and laundries [51]. Some articles have documented DDBAC concentrations in natural aquatic environments, reporting values in the range of 0.05 to 6 mg L^{-1} in effluents from European hospitals before the 2019 pandemics [42].

While the literature regarding the effects of ALAN on urban biodiversity is growing, its impacts on aquatic biodiversity remains less investigated, especially with regards to its combination with other types of urban stresses, particularly chemical contamination, on aquatic primary producers. Within primary producers, aquatic biofilms are ubiquitous in aquatic environments [40] and constitute a dynamic community with very diverse microorganisms composing them [81]. Biofilms play a very important role in aquatic ecosystems, participating in primary production or carbon cycling [15]. Freshwater biofilms are generally dominated by cyanobacteria, diatoms and green algae (e.g [61]). The photosynthetic activity of their microalgal constituents can be impacted by excess light exposure, with the generation of reactive oxygen species, as demonstrated by Waring et al. [90], Cheloni et al. [12] or Erickson et al. [19]. ALAN can also lead to dysregulation of circadian cycles and consequently impair the photosynthesis in biofilm microalgae [19,48,90]. The impact of DDBAC on the photosynthesis of freshwater biofilms was also documented by Vrba et al. [87]. They tested the short-term inhibition of the photosynthesis of natural biofilms after a 4-hour exposure to increasing concentrations of DDBAC. They determined an EC5 (Effective concentration inducing a 5% decrease in photosynthesis) of 30 mg L^{-1}, which was further established in their work as the nominal concentration for chronic exposure of the biofilms. At this elevated concentration, they found striking effects on the photosynthesis and health of algal cells [87] as well as on lipid profiles [53].

Biofilms are a source of nutrients for higher organisms such as invertebrate or vertebrate grazers, providing them with some essential fatty acids (FA) produced by microalgae, which are rich in omega 3 and omega 6 [82]. The transfer of FA from microalgae in biofilms to higher trophic levels is therefore crucial for the functioning of aquatic food webs [23,66,78]. In cells, FA contribute to the maintenance of membrane fluidity and have a central role in the storage of metabolic energy [37,54]. FA have a structural role in cells, being present in cell membranes as phospholipids [35] and glycolipids [8]. FA profiles allow the determination of taxonomic groups [94]. For example, diatoms are rich in C20:5 [8], essential for consumers [83]. Reserve FAs from triacylglycerides (TAG) serve as a form of carbon and energy storage, for example, under conditions of environmental stress [37]. In microalgae, both FA composition and the presence of oxylipins proved to be good indicators of toxic stress [16,23,74]. Oxylipins can indeed denote oxidative stress in cells, for example HODEs (hydroxyoctadecadienoic acids), HOTrEs (hydroxyoctadecatrienoic acids), HETEs (hydroxyeicosatetraenes acids) and HEPEs (hydroxyeicosapentaenoic acids) which respectively derive from the oxidation of linoleic acid (C18:2), octadecatrienoic acid (C18:3), arachidonic acid (C20:4) and eicosapentaenoic acid (C20:5).

In this context, an experimental approach under controlled conditions was implemented to understand the effects of two stressors specific of urban environments (ALAN exposure and chemical contamination by DDBAC) on aquatic biofilms. In this experiment, we tested for the influence of continuous light vs. day/night alternation, and the effect of an environmental nominal contamination of dissolved DDBAC (100 µg L^{-1}, [3]). Several functional and structural descriptors were used. The functional descriptors mainly relate to biofilm photosynthesis, which was expected to be impaired by urban pollutants. Structural descriptors such as the FA composition of the biofilms and oxylipin content were also assessed.

2. Materials and methods

2.1. Pre-exposure conditions

2.1.1. Biofilms

Clean glass slides were immersed in the Cestas-Gazinet pond (lat.: 44.774601; long.: −0.696077) for biofilm colonization. Their dimensions were of 217 ± 20 cm^2. Colonization took place from 12/14/22 to 02/22/23, during the winter period under hypereutrophic water conditions [11].

2.1.2. DDBAC

The benzyldimethyldodecylammonium chloride used (DDBAC, powder form; CAS: 139–07-1, purity > 99%) was purchased from Sigma Aldrich, France. A stock solution of DDBAC was prepared at 100 mg L^{-1} in Ultra Pure Water. The stock solution was further used to contaminate the water in the experimental beakers, to reach a nominal concentration of 100 µg L^{-1} at the beginning of the exposure, then every 2–3 days on the occasion of water changes (see Section 2.2).

2.2. Experimental setup

The experiment lasted one month, from 02/22/23 to 03/24/23. The effects of light exposure at night and chemical exposure to DDBAC were tested individually and jointly, in 4 experimental conditions, each performed in triplicate independent beakers. For light conditions, two contrasted photoperiods were used: an alternate photoperiod (AP) of 10 h day and 14 h night, corresponding to the natural photoperiod during biofilm colonization *in situ*, and a continuous photoperiod (CP) where light exposure was continuous over 24 h. Artificial light was provided by aquarium LEDs (JBL LED SOLAR NATUR 37 W; 4000 K; PAR = 223 µM s^{-1} m^{-2}, supplier's manual). DDBAC contamination was carried out at a nominal concentration of 100 µg L^{-1} [3]. The conditions tested will be thereafter referred to as AP_Ctrl, AP_BAC, CP_Ctrl and CP_BAC.

Once the *in situ* colonization of the glass slides by biofilms was achieved, 7 slides were collected and considered as the initial day (D0) control. 24 more colonized slides were introduced into 8-liter beakers of medium (2 slides per beaker). The culture medium was prepared in mineralized water enriched with nutrients, close to the conditions prevailing in the pond during the colonization period. Its detailed composition is provided in Table 1.

Every two to three days, water renewals were carried out and the physicochemical composition of the medium was monitored (see Section 2.3.1). After 14 days of exposure (D14), one slide of each beaker was harvested. Then after 30 days of exposure (D30), the remaining slides were recovered. For each biofilm slide, a surface area of 34 ± 13 cm^2 was scraped and suspended in 4 mL of beaker's water for subsequent PhytoPAM analyses (see Section 2.4.1). Then, the slides covered by a remaining biofilm surface area of 183 ± 20 cm^2 were quenched with liquid nitrogen and freeze-dried for lipid analyses (see Section 2.4.2).

2.3. Water analyses

2.3.1. Physico-chemical parameters

Twice a week, the water pH, dissolved oxygen saturation, conductivity and temperature were monitored using appropriate probes (pH and temperature Sentix 41, Cellox 325 and Tetracon 325). The incident photosynthetically active radiation (PAR) measurements were carried out at the end of the experiment in the air on the surface and near the beakers, and in the water at the level of the biofilm slides, using a luxmeter LI-1935A (Biosciences GmbH). Anion (nitrite, nitrate, phosphate, sulfate and chloride) and cation (ammonium, sodium, potassium, calcium and magnesium) analyses were carried out by Ion Chromatography (881 Compact IC pro 1). For this purpose, 20 mL of beaker water were collected, filtered with 26 mm (diameter) and 0.45 µm (porosity) PTFE syringe filter (Phenomenex, Phenex), stored at 4 °C and analyzed within 3 days. Anion concentrations were measured before every regular water change while cations were analyzed at the beginning and at the end of the experiment.

2.3.2. DDBAC concentrations

Concentrations of DDBAC were measured in the water at the start of the exposure, after 1, 2, 6, 24 h of exposure and then every day until the end of the experiment. A minimum volume of 1.5 mL was collected and stored at − 20 °C. Water samples were filtered with 26 mm (diameter) and 0.45 µm (porosity) PTFE syringe filters (Phenomenex, Phenex). Then, 200 µL water samples, spiked with 2 µL of DDBAC-d5 (10 µg mL^{-1}) as internal standard, were injected into a Dionex Ultimate 3000 HPLC (Thermo Fisher Scientific, France) coupled with an API 2000 triple quadrupole mass spectrometer (Sciex, France). A Gemini® NX-C18 column from Phenomenex was used as a stationary phase. The mobile phase was 90:10 5 mM acetonitrile/water. The analysis was performed in isocratic mode, i.e. the composition of the mobile phase was kept constant during the analysis, as described in Vrba et al. [87]. The quantification limit was of 0.2 ng mL^{-1}.

2.4. Biofilm analyses

2.4.1. Fluorescence-based analyses on fresh biofilm suspensions

The effective photosynthetic yield [30] and chlorophyll fluorescence of the 4 mL biofilm suspensions (corresponding to a glass slide surface of

Table 1
Summary of average exposure conditions (mean ± standard errors) during the experiment. Different superscript letters indicate statistical differences between individual conditions ('All'; Kruskall Wallis test) or specific effect of either ALAN or DDBAC (Wilcoxon-Mann-Whitney test). Quantification limits are provided with the same unit and precision as the corresponding measurement values.

	Conditions	n	Mean ± SE	Quantification limit
pH	All	30	7.7 ± 0.1	N/A
Oxygen (%)	All	25	108.6 ± 4.7	N/A
Conductivity (µS cm^{-1} at 25 °C)	All	30	687 ± 19	N/A
Water temperature (°C)	AP	18	22.0 ± 0.1^a	N/A
Water temperature (°C)	CP	12	22.8 ± 0.2^b	N/A
NO_2 (mg L^{-1})	All	36	0.16 ± 0.03	0.005
NO_3 (mg L^{-1})	All	36	19.41 ± 1.02	0.01
PO_4 (mg L^{-1})	All	36	0.03 ± 0.01	0.01
SO_4 (mg L^{-1})	All	36	123.24 ± 4.88	0.005
Cl (mg L^{-1})	All	36	55.88 ± 2.83	0.01
NH_4 (mg L^{-1})	All	12	0.15 ± 0.03	0.005
Na (mg L^{-1})	All	12	62.28 ± 5.59	0.01
K (mg L^{-1})	All	12	6.85 ± 1.19	0.0025
Ca (mg L^{-1})	All	12	38.72 ± 8.26	0.15
Mg (mg L^{-1})	All	12	6.95 ± 0.57	0.15
$[DDBAC]_{water}$ (µg L^{-1})	Abiotic control	30	8.9 ± 1.7^a	0.2
$[DDBAC]_{water}$ (µg L^{-1})	DDBAC	188	1.2 ± 0.3^b	0.2
Incident light in the water (µmol m^{-2} s^{-1})	All	16	148 ± 8	N/A
$[DDBAC]_{biofilm}$(ng mg^{-1})	J0	7	0.0 ± 0.0^a	0.2
$[DDBAC]_{biofilm}$(ng mg^{-1})	Ctrl	12	0.0 ± 0.0^a	0.2
$[DDBAC]_{biofilm}$(ng mg^{-1})	DDBAC	12	1 ± 0.2^b	0.2

N/A: non applicable.

34 ± 13 cm^2) were measured using a PhytoPAM fluorimeter (Heinz Walz GmbH, Germany). The biofilm suspensions were acclimated to the measuring light for approximately 4 h in the laboratory at 22 °C, before the samples were placed for analyses in a quartz cuvette agitated by a stirring rod. The PAR used for measurements was of 164 µmol quanta m^{-2} s^{-1}. The PhytoPAM analyses were performed for each sample, in technical triplicates, which were averaged afterwards. For ease of biofilm data comparisons, the chlorophyll fluorescence data are expressed below in ng mg^{-1} dry weight biofilm.

2.4.2. Freeze-dried biofilms pre-processing

After quenching and freeze-drying, the biofilm samples (10–20 mg dry mass) were weighed using a Mettler Toledo NS204S analytical balance and placed in 2 mL microtubes containing 150 mg of microbeads. The single-phase solid-liquid extraction procedure involved the addition of 1 mL of a mixture of MTBE (Methyl tert-butyl ether):EtOH (ethanol), 3:1 (v/v) and 0.01% BHT (butylhydroxytoluene). Before extraction, 50 µL of a PE (phosphatidylethanolamine) solution (15:0/15:0) containing 100 ng $µL^{-1}$ was added as a standard and 5 µL of a C17:0 solution at 1000 ng $µL^{-1}$. The samples containing microbeads were mechanically homogenized and extracted (3 cycles of 15 s) with the solvent using an MP Biomedicals FastPrep-24 5 G. The supernatant was separated from the pellet (containing biological material and microbeads) by centrifugation at 12,000 rpm. At this stage, 800 µL of this organic solvent phase were retrieved. A second extraction step (3 cycles of 15 s and centrifugation) was carried out after adding 1 mL of MTBE:EtOH, 1:1 (v/v) and 0.01% BHT mixture to the pellet and centrifugating as previously. One mL of supernatant was collected again and added to the previous one to form the lipid extract, stored at − 80 °C. Details on the entire extraction procedure can be found in Mazzella et al. [52]. Prior to analysis, the solvent was evaporated under a nitrogen flow and the samples were further diluted in MTBE (typical volume 1 mL), stored at − 18 °C and analyzed within 1 week, prior to the fractionation step. Different aliquots were used to quantify the DDBAC concentration in the biofilms, free lipid content, and relative concentrations of fatty acids from structure/storage lipids after fractionation and saponification.

2.4.3. Analyses performed on the free lipid fraction

2.4.3.1. DDBAC bioaccumulated in biofilms. Following solid-liquid extraction, DDBAC concentration in the biofilms was quantified with 200 µL of the sample and 2 µL of DDBAC d5 solution of 10 ng $µL^{-1}$, following the same protocol as used for water samples (see Section 2.3).

The results were then expressed as log10 value of the bioconcentration factor (i.e. log(BCF)). The BCF was calculated according to the following formula:

$$\mathrm{BCF} = \frac{DDBAC\ concentration\ in\ biofilm(\mu g \quad kg^{-1})}{DDBAC\ concentration\ in\ water(\mu g \quad L^{-1})} \tag{1}$$

2.4.3.2. Oxylipins. Oxylipins (HODEs: hydroxyoctadecadienoic acids, HOTrEs: hydroxyoctadecatrienoic acids, HETEs: hydroxyeicosatetraenes acids and HEPEs: hydroxyeicosapentaenoic acids) were measured on the free lipid fraction. The samples were analyzed using an Ultimate 3000 HPLC coupled with an API 2000 triple quadrupole mass spectrometer. A Kinetex C8 (2.8 µm, 100 × 2.1 mm) column from Phenomenex was used as a stationary phase. The analysis was performed in isocratic mode, with a mobile phase of 50:50 5 mM acetonitrile/isopropanol. The flow rate was 300 µL min^{-1}, the injection volume was 20 µL. The limit of quantification is 5 ng mL^{-1}.

The standards used were composed of 9(S)-HOTrE (9S-hydroxy-10E,12Z,15Z-octadecatrienoic acid, Cayman chem, France; CAS: 89886–42-0, purity > 98%); 9-HODE ((±)− 9-hydroxy-10E,12Z-octadecadienoic acid, Cayman chem, France; CAS: 98524–19-7, purity > 98%); (S)− 12-HETE (12(S)-Hydroxy-(5*Z*,8*Z*,10*E*,14*Z*)-eicosatetraenoic acid, sigma aldrich, USA; CAS:54397–83-0, purity ≥ 95%). The standards were used for both calibration range and detection settings. The internal standards used were 13(S)-HODE-d4 (13S-hydroxy-9Z,11E-octadecadienoic-9,10,12,13-d4 acid; Cayman chem, France; CAS: 139408–39-2, purity > 99%); (±)-Jasmonic Acid-d5 (3-oxo-2-(2Z)2-penten-1-yl-cyclopentane-2,4,4-d3-acetic-2,2-d2 acid; Cayman chem, France; CAS: 2750534–78-0, purity > 99%). These were added to 200 µL of sample, 10 µL of 0.1 ng $µL^{-1}$ 13(S)-HODE-d4 and 2 µL of 2.5 ng $µL^{-1}$ Jasmonic Acid-d5.

The oxylipin ratio was calculated as

$$\frac{\sum Concentrations\ of\ oxylipins}{Concentration\ of\ free\ lipid\ fraction} \tag{2}$$

and expressed as per thousand.

2.4.4. Fatty acids from membrane-forming and storage lipids

The membrane lipids (polar lipids, as phospholipids and glycolipids) and storage lipids (neutral lipids, as triglycerids) were fractionated using chromatography carried out on 1 g Silica SPE extraction cartridges (Waters) following a protocol adapted from Hamilton and Comai, [33]. The sample was loaded on the top of the cartridge and eluted successively with MTBE (Methyl tert-butyl ether, 10 mL) and MeOH (methanol, 10 mL). The first fraction (F1) was neutral lipids, which contained storage lipids, and the second fraction (F2) contained polar lipids. Each of the two fractions was dried under nitrogen and 300 µL of MeOH was added. For each of the fractions, 150 µL were collected for saponification, using 10 µL Me-C19:0 (Methyl nonadecanoate; Merck; CAS: 1731–94-8; purity > 98%) at 100 mg L^{-1} as surrogate. One mL of 1 M sodium hydroxide was added and then heated to 80 °C for 30 min using a Hisorb stirrer (Markes). Once the mixture had cooled, 100 µL formic acid and 1 mL MTBE were added. After a 1 min centrifugation at 3000 rpm, with an EBA 20 Hettich Bench Top Centrifuge, 500 µL of the solution was recovered, and the solvent was evaporated to dryness under a nitrogen flow. The sample was then diluted in 1 mL Ultra Pure Water/Acetonitrile (90:10) and stored at − 20 °C until analysis. Both fatty acid and oxylipin analyses were performed using a Dionex Ultimate 3000 HPLC (Thermo Fisher Scientific, France) coupled with an API 2000 triple quadrupole mass spectrometer (Sciex, France) with a Kinetex C8 (2.8 µm, 100 × 2.1 mm) column. The mobile phase was acetonitrile (ACN)/isopropanol 50/50 (more details in suppl mat table S1, S2, S3 and S4).

2.5. Data analyses

Data visualizations and statistical analyses were carried out using R (4.0.4) and R studio (2022.12.0 Build 353). Data are presented as average values ± standard errors (with package *plotrix*). Temporal changes in fatty acid composition between D0 and D30 were described through Principal Component Analyses performed with *FactoMineR* package, illustrating the grouping of individual values among treatments with convex hulls. Statistically significant differences between conditions (AP_Ctrl, AP_BAC, CP_Ctrl and CP_BAC) were highlighted using Kruskall-Wallis tests, followed when necessary by Dunn post-hoc tests. To assess the effects of ALAN and DDBAC on biofilm descriptors, Wilcoxon-Mann-Whitney tests were carried out. A p-value below 0.05 was considered as significant.

3. Results

3.1. Experimental conditions

Average physicochemical values are provided in Table 1. The physicochemical parameters in the experimental systems were similar

between conditions over time (Kruskall-Wallis test, p-value > 0.05). The water temperature was significantly higher in CP conditions than in AP conditions (Wilcoxon test, p-value < 0.05); however, this difference was of less than 1 °C in average.

DDBAC concentrations in the abiotic control were one order lower than expected (8.94 ± 1.74 μg L^{-1}) throughout the 21 first days of the experiment, then drastically decreased to barely quantifiable levels (Table 1, Fig. S5). DDBAC concentrations in the water of the conditions including biofilms were even lower than the abiotic control (p-value < 0.05). DDBAC concentrations were highly variable over time and averaged 1.2 ± 0.3 μg L^{-1}, for all experimental conditions and sampling times (N = 188). A sharp decrease in DDBAC concentrations was observed over the first day of experiment in all conditions (p-value < 0.05, Dunn test; Fig. S5), and did not increase again after water renewals. However, under DDBAC conditions, the contaminant was quantified in the biofilms (0.98 ± 0.18 ng mg^{-1} biofilm, N = 12) showing stable sorption between D14 and D30, while D0 and control biofilms were free of DDBAC (p-value < 0.05; Dunn test). Biofilms exposed to DDBAC exhibited a log(BCF) of 2.97 ± 0.16 all dates combined.

3.2. Biofilm functional descriptors

3.2.1. Effective quantum yield

The photosynthetic yield of the biofilm inoculum (D0) averaged 0.43 ± 0.03 (Fig. 1). Similar values were recorded on D14 (0.43 ± 0.02), while significantly lower yields (0.27 ± 0.02) were measured on D30 (p-value < 0.05, Dunn test).

Considering all dates, photosynthetic yields were significantly higher in AP conditions than in CP conditions (p-value < 0.05, Wilcoxon test; AP: 0.41 ± 0.02 vs. CP: 0.32 ± 0.03). Such influence of light conditions on the yield was still observable on D30, where AP values exceeded those of CP biofilms (p-value < 0.05, Wilcoxon test; on D30, AP: 0.32 ± 0.07 vs CP: 0.23 ± 0.07).

3.2.2. Fluorescence-based chlorophyll-a concentrations

Fluorescence-based chlorophyll *a* concentrations in the biofilm inoculum (D0) were of 7 ± 2 ng mg^{-1} dry weight biofilm (Fig. 2). Overall, chlorophyll *a* fluorescence significantly increased from D0 to D14, reaching 34 ± 6, then decreased to 10 ± 3 ng mg^{-1} on D30 (p-value < 0.05, Dunn test). No significant differences in chlorophyll *a* content were highlighted between conditions.

3.2.3. Proportions of algal groups

The biofilm used in the experiment was initially (D0) dominated by green algae (61 ± 2 %) followed by 30 ± 3 % of cyanobacteria and 10 ± 2 % of diatoms (Fig. 3).

The proportion of green algae gradually decreased over time in all conditions (p-value < 0.05, Dunn test; D14: 44 ± 5 % and D30: 38 ± 4 %), while the relative abundance of diatoms increased (p-value < 0.05, Dunn test; D14: 37 ± 7 % and D30: 38 ± 4 %). The proportion of cyanobacteria halved between D0 and D30 (p-value < 0.05, Dunn test; D30: 13 ± 1 %).

The composition of the biofilm significantly differed according to the prevailing light conditions. The proportion of green algae was higher in AP than CP conditions (p-value < 0.05, Wilcoxon test, AP: 53 ± 3 % vs. CP: 33 ± 4 %), while diatoms were significantly more abundant under CP compared to AP conditions (p-value < 0.05, Wilcoxon-Mann-Whitney test; AP: 29 ± 4 %, CP: 46 ± 4 %).

3.3. Lipid descriptors

3.3.1. Fatty acids from membrane lipids

On D0, total membrane lipid (i.e. both phospholipids and glycolipids like polar lipids) content averaged 46.71 ± 9.41 nmol mg^{-1} dry weight biofilm. Considering these lipids according to the saturation degree of their ester-linked fatty acids, biofilms contained high amounts of PUFA (36.68 ± 7.84 nmol mg^{-1}; Table 2) and lower quantities of SFA and MUFA (SFA: 4.32 ± 0.46 nmol mg^{-1}, MUFA: 5.72 ± 1.19 nmol mg^{-1}).

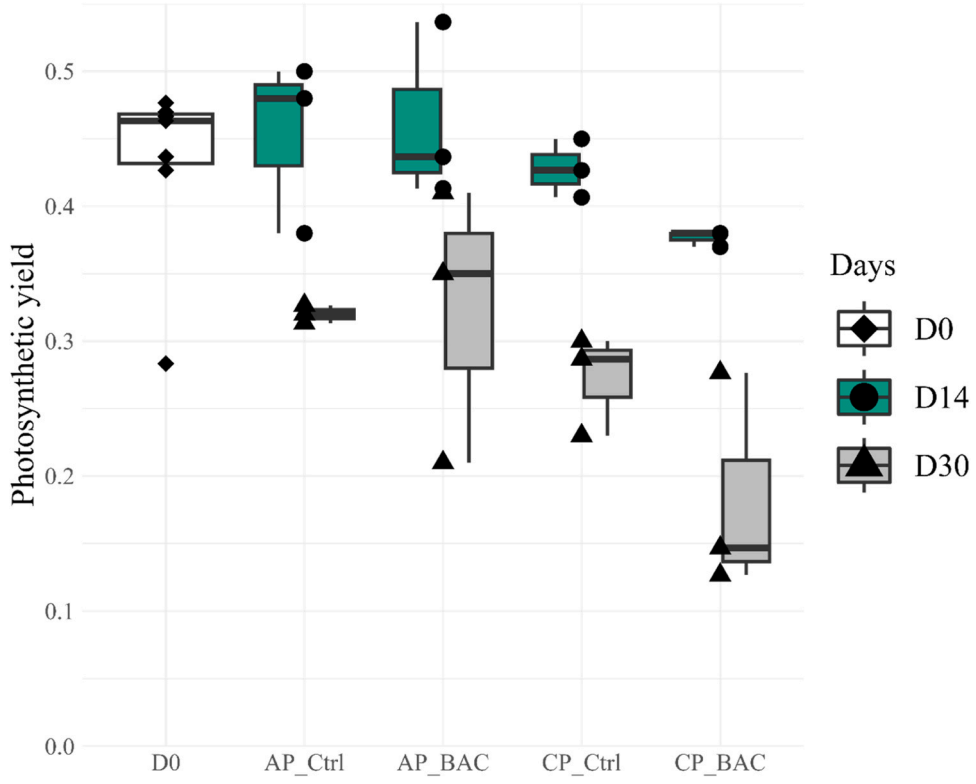

Fig. 1. Photosynthetic yield (relative values) measured for each experimental condition after various exposure durations (Day 0-D0: diamonds, white; Day 14-D14: dots, green; Day 30-D30: triangles, gray). AP: Alternate photoperiod, CP: Continuous photoperiod, with DDBAC when BAC is indicated.

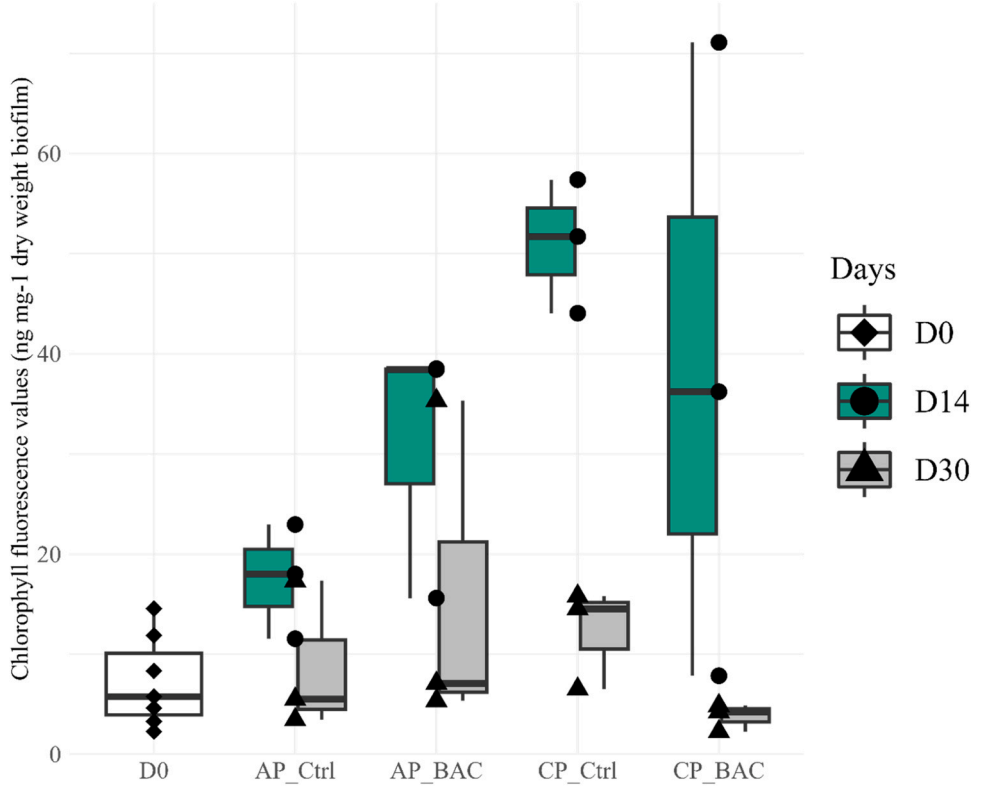

Fig. 2. Chlorophyll fluorescence values (ng mg^{-1} dry weight biofilm), as a function of the experimental conditions and exposure duration (Day 0-D0: diamonds, white; Day 14-D14: dots, green; Day 30-D30: triangles, gray). AP: Alternate photoperiod, CP: Continuous photoperiod, with DDBAC when BAC is indicated.

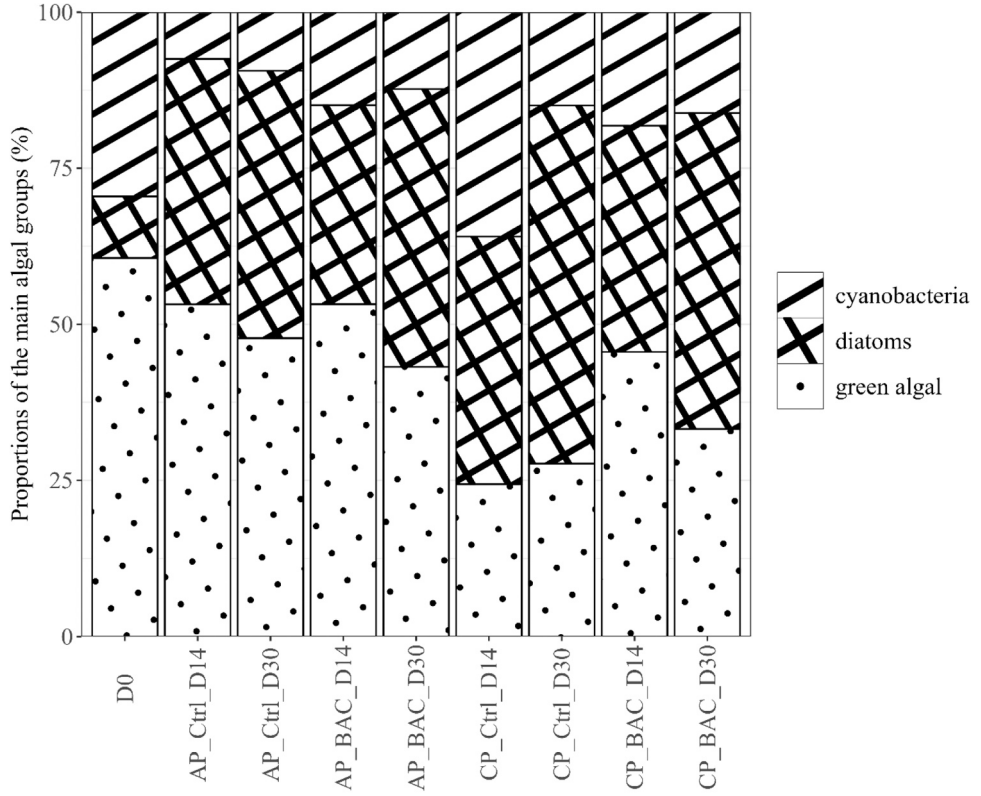

Fig. 3. Proportions of the main algal groups in the biofilm based on the relative fluorescence of blue, green and brown microalgae, as a function of the experimental conditions and exposure duration (Day 0-D0, Day 14-D14, Day 30-D30). AP: Alternate photoperiod, CP: Continuous photoperiod, with DDBAC when BAC is indicated, Note that total concentrations of chlorophyll a (corresponding to all microalgae) differed between dates and treatments as shown in Fig. 2.

The quantity of total membrane lipids was stable between D0 and D14 (46.06 ± 6.49 nmol mg^{-1}) but drastically decreased on D30 (23.68 ± 4.59 nmol mg^{-1}; p-value < 0.05, Dunn test). There was no difference between experimental conditions (p-value > 0.05, Kruskall test).

The PCA carried out on the data set of membrane lipid abundances (%) at D0 and D30 made it possible to explain 69.1% of the variance in the lipid composition of the biofilms (Fig. 4). Fig. 4B highlights a clear distinction between samples under AP conditions without DDBAC exposure and the other conditions (p-value < 0.05, Dunn test) along Axis 1 (40.9% of the variance) and a distinction between days D0 and D30 in terms of specific fingerprint based on biofilm membrane lipids along Axis 2 (28.2%).

Indeed, the inoculum (D0) was characterized by higher proportions of C16:4 (15.29 ± 1.02 %), C18:3 (23.57 ± 5.14 %), C18:4 (5.14 ± 0.40 %), and C20:3 (1.00 ± 0.21 %) (Fig. 4A). On D30, under control conditions (AP without DDBAC exposure), the biofilms had greater content of C12:0 (3 ± 2.08 %), C14:0 (7.67 ± 2.73 %), C16:0 (15.33 ± 2.33 %), and C22:4 (1 ± 1 %). Membrane lipid content under the other tested conditions highlighted divergence related to specific fatty acids such as C16:1 (AP_BAC: 11 ± 1.73 %; CP_Ctrl: 15 ± 2.08 %; CP_BAC: 15 ± 2.08 %), C18:1 (AP_BAC: 13 ± 0.60 %; CP_Ctrl: 12.33 ± 0.67%; CP_BAC: 12.33 ± 2.02 %), C18:2 (AP_BAC: 13 ± 1 %; CP_Ctrl: 11.33 ± 0.88 %; CP_BAC: 13.66 ± 1.45 %), C20:4 (AP_BAC: 6.33 ± 0.33 %; CP_Ctrl: 10.67 ± 1.33 %; CP_BAC: 7 ± 1 %) and C20:5 (AP_BAC: 16.67 ± 1.86 %; CP_Ctrl: 17 ± 2.31 %; CP_BAC: 14.33 ± 1.76 %).

3.3.2. Fatty acids from storage lipids

Storage lipids (i.e. TAG like neutral lipids) in the inoculum (D0) accounted for 16.24 ± 1.22 nmol mg^{-1} dry weight biofilm, with 9.87 ± 0.69 nmol mg^{-1} of PUFA, 3.34 ± 0.23 nmol mg^{-1} of SFA and 3.04 ± 0.32 nmol mg^{-1} of MUFA (Table 3). The total quantities of storage lipids increased on D14 (88.25 ± 52.59 nmol mg^{-1}) then decreased dramatically on D30 (9.86 ± 1.52 nmol mg^{-1}), with a significant effect of exposure duration (p-value < 0.05, Dunn test). Moreover, lipid reserves were significantly lower in Ctrl conditions compared to biofilms exposed to DDBAC (p-value < 0.05, Wilcoxon test; Ctrl: 28.34 ± 8.92 nmol mg^{-1} vs. DDBAC: 63.72 ± 53.24 nmol mg^{-1}).

Changes in fatty acids occurred over the experiment, and highlighted an effect of DDBAC exposure. As observed for total storage lipids, PUFA content increased over the first 2 weeks (D14: 36.35 ± 21.14 nmol mg^{-1}) then dropped down to 3.88 ± 0.69 nmol mg^{-1} on D30 (p-value < 0.05, Dunn test). PUFAs were significantly lower (p-value < 0.05, Dunn test) under AP_BAC 1.76 ± 0.0.38 nmol mg^{-1} than Ctrl conditions (AP_Ctrl: 13.17 ± 4.28 nmol mg^{-1}) or under continuous photoperiod conditions (CP_BAC: 49.70 ± 42.34 nmol mg^{-1}).

Similar patterns were observed for MUFAs. On D14, MUFA concentrations (33.53 ± 20.64 nmol mg^{-1}) were significantly higher compared to D0 then decreased on D30 (3.20 ± 0.55 nmol mg^{-1}), confirming the effect of timing (p-value < 0.05, Dunn test). DDBAC-exposed biofilms had greater MUFA content under continuous illumination (CP_BAC: 46.99 ± 41.23 nmol mg^{-1}) compared to alternate photoperiod conditions (AP_BAC: 1.47 ± 0.37 nmol mg^{-1}) (p-value < 0.05, Dunn test).

The PCA shown in Fig. 5 is based on storage lipid data analyzed on D0 and D30; the analysis describes 54.3 % of the variance in the composition of biofilms related to inter-conditions and temporal changes. Fig. 5B highlights a clear temporal distinction between days D0 and D30, along Axis 1 (34.8 %). Axis 2 of the PCA (19.5 %) individualizes AP_BAC at D30, however, the dispersion of individuals did not allow to evidence statistically significant differences.

The storage lipid content varied over time: in fact, at D0, there were more C16:4 (14.28 ± 0.39 %), C18:3 (11.98 ± 0.68 %), C18:4 (6.4 ± 0.50 %), C22:5 (0.67 ± 0.04 %). However, at D30, there were more C16:0 (15.59 ± 0.80 %) and C16:1 (17.02 ± 1.46 %).

Also, storage lipid content in AP_BAC biofilms versus the other tested conditions highlighted divergences related to specific fatty acids such as C16:0 (18.17 ± 0.70 %), C18:0 (10.40 ± 0.60 %); C18:1 (13.93 ± 1.42 %); C20:0 (4.77 ± 1.45 %); C22:4 (0.17 ± 0.03 %) for AP_BAC. AP_BAC biofilms contained more saturated FAs (C16:0 and C18:0) than in CP_BAC, highlighting the effect of light changes. In contrast, CP_BAC biofilms contained more C16:1 (16.70 ± 3.43 %), C14:0 (5.20 ± 0.50 %) and C20:4 (2.67 ± 0.67 %).

Table 2
Summary of membrane lipids concentrations (mean ± standard errors) during the experiment in nmol mg^{-1}.

Days	Total membrane lipids	SFA	MUFA	PUFA
D0	46.71 ± 9.41	4.32 ± 0.46	5.72 ± 1.19	36.68 ± 7.84
D14	46.06 ± 6.49	3.30 ± 0.51	7.07 ± 0.91	35.69 ± 5.33
D30	23.68 ± 4.59	4.02 ± 0.95	5.81 ± 1.29	13.85 ± 2.98

3.4. Oxylipins as markers of oxidative stress

HEPE (hydroxyl-pentaenoic acids) and HETE (hydroxy-eicosatetraenes acids), deriving from the oxidation of eicosapentaenoic acid (C20:5) and arachidonic acid (C20:4), were not present in our samples despite the presence of C20:5 and C20:4 (Figs. 4 and 5; [79]). The oxylipins HODEs and HOTrEs identified were analyzed from the free fatty acids fraction, and may thus be considered as a global lipid stress/oxidation, not affecting storage or membrane lipids (Fig. 6). On D0, the concentrations of oxylipins were 5.39 ± 4.96 pmol mg^{-1} of HODEs and 3.23 ± 2.70 pmol mg^{-1} of HOTrEs, with an oxylipin ratio of 0.43 ± 0.38 ‰. A significant increase in oxylipin concentrations and oxylipin ratio was observed between D0 and D30 (p-value < 0.05, Dunn test; D30: 2.50 ± 0.66 ‰). At the end of the experiment, HODE concentrations reached 36.97 ± 6.15 pmol mg^{-1}, and HOTrE levels were 7.70 ± 1.43 pmol mg^{-1}, leading to an oxylipin ratio of 2.50 ± 0.66 ‰.

For all oxylipin descriptors, a significant impact of DDBAC exposure was highlighted. HODE concentrations in the biofilms exposed to DDBAC were significantly higher than under Ctrl conditions all times combined (p-value < 0.05, Wilcoxon test, DDBAC: 35.46 ± 7.63 pmol mg^{-1} vs. Ctrl: 16.27 ± 3.97 pmol mg^{-1}). A significant increase in HOTrE concentrations under DDBAC exposure was observed on D14 only (p-value < 0.05, Wilcoxon test, DDBAC: 8.73 ± 3.03 pmol mg^{-1} vs. Ctrl: 1.66 ± 0.91 pmol mg^{-1}). As a consequence, the ratio oxylipins/total fatty acids was significantly higher with DDBAC exposure than under Ctrl conditions (p-value < 0.05, Wilcoxon test, DDBAC: 2.50 ± 0.67 ‰ vs. Ctrl: 0.87 ± 0.25 ‰). This significant difference was observed from D14, where Ctrl values were already lower than DDBAC-exposed ratios (p-value < 0.05, Wilcoxon test, Ctrl: 0.48 ± 0.24‰ and DDBAC_D14: 1.78 ± 0.45 ‰).

4. Discussion

This experiment consisted in characterizing the effects of two urban pollutants: ALAN and DDBAC, on freshwater biofilms using different biomarkers. The experimental environments were similar between exposure conditions and stable over the experiment, except for water temperature which was about 0.8 °C higher under continuous illumination compared to the alternate photoperiod (CP: 22.77 ± 0.22 °C; AP: 21.99 ± 0.09 °C). This difference can be explained by the continuous lighting of the LEDs, which probably affected the temperature. Such a slight increase in temperature is unlikely to significantly drive the response of the descriptors studied here. In Yang et al. [93], there was no significant effect on polysaccharide content between 25 and 30 °C. The experimentation of Hua et al. [38] did not study temperature variation, but their range of values was greater than ours (17 to 25 °C, vs. 22 to 23 °C in this study). Therefore, the results presented here were mostly related to the alteration of photoperiod or DDBAC contamination.

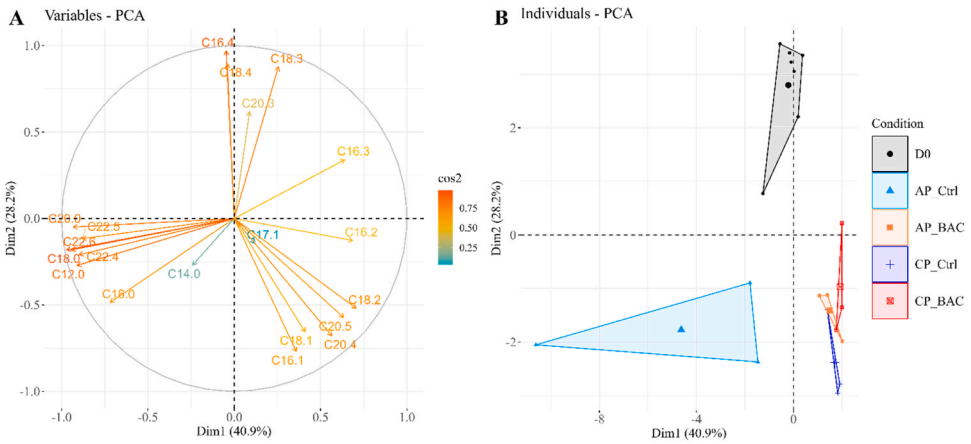

Fig. 4. Principal Component Analysis (PCA) carried out on the relative abundance of fatty acids (%) in membrane lipids, as a function of experimental conditions (AP: Alternate photoperiod, CP: Continuous photoperiod, with BAC when indicated) and sampling dates (D0 vs. D30). A: Correlations between variables (fatty acids relative concentrations) on dimensions 1 and 2; B: Projection of the observations, grouped by conditions (D0: black dots, AP_Ctrl: gray triangles, AP_BAC: pink squares, CP_Ctrl: blue crosses, CP_BAC: purple squares) on the same dimensions.

Table 3
Summary of storage lipids concentrations (mean ± standard errors) during the experiment in nmol mg^{-1}.

Days	Total storage lipids	SFA	MUFA	PUFA
D0	16.24 ± 1.22	3.34 ± 0.23	3.04 ± 0.32	9.87 ± 0.69
D14	88.25 ± 52.59	18.37 ± 10.84	33.53 ± 20.64	36.35 ± 21.14
D30	9.86 ± 1.52	2.85 ± 0.34	3.20 ± 0.55	3.81 ± 0.69

4.1. ALAN impacts on biofilms

In the literature, ALAN has already been shown to influence the mechanisms of photosynthetic activity and competitive interactions between the species composing biofilms [32,49,50]. In this study, ALAN caused a reduction in the photosynthetic yield of biofilms, confirming the impact of continuous illumination on the photosynthesis cycle and associated ecosystem functions [49]. Photosynthesis consists in the optimal absorption of light: in the chloroplast, the incident photon flux is harvested by specific proteins located in photosystem II (PSII) and the electron transport through the thylakoid membrane is further used for ATP synthesis [39]. Excess light exposure destabilizes the transthylakoid pH gradient by proton accumulation in the lumen, potentially driving reactive oxygen species (ROS) production and damaging the photosynthetic apparatus [4]. In natural conditions, different processes can reduce the impact of excessive or continuous light on the biofilm and ensure photoprotection. High intensity light is known to induce photoinhibition and photodamage [19,39,90]. It provokes a sharp decrease in photosynthetic efficiency, followed by a rapid recovery of the original photosynthetic levels [71], suggesting the capacity to quickly initiate photoprotective mechanisms. Photoprotection against high irradiances is achieved in photosynthetic organisms through several complementary mechanisms, such as the thermal dissipation of excess energy stimulated by the proton-induced xanthophyll cycle (non-photochemical quenching) or the production of antioxidant or scavenging enzymes to deal with excess ROS [65]. In our study, different hypotheses could explain the reduction in photosynthetic yield under ALAN conditions: a decrease in the size of the light-harvesting complexes, changes in the compositions and concentrations of pigments, saturation of the electron transport chain [39,48,80]. A study on the cyanobacteria *Microcystis aeruginosa* in the presence of ALAN showed, for example, an increase in chlorophyll *a* content and a reduction in the number of PSI per chlorophyll *a* [67]. At this point, complementary studies are necessary to validate or not these hypotheses on a multi-specific community.

A likely consequence of inter-species differential abilities to cope with photodamage, ALAN impacts the taxonomic composition of primary producers, as highlighted by Hölker et al. [36], Grubisic et al. [32]

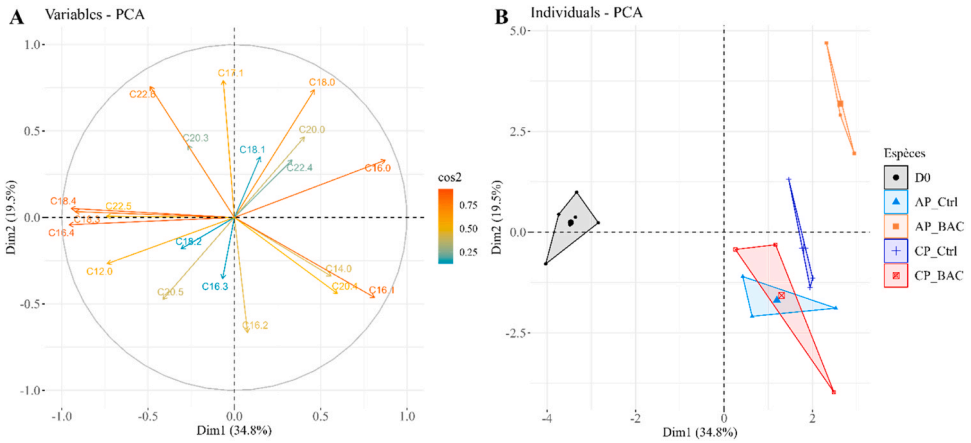

Fig. 5. Principal Component Analysis (PCA) carried out on the relative abundance of fatty acids (%) in storage lipids, as a function of experimental conditions (AP: Alternate photoperiod, CP: Continuous photoperiod, with DDBAC when indicated) and sampling dates (D0 vs. D30).A: Correlation circle of the variables (fatty acids) on dimensions 1 and 2B: Projection of the observations, grouped by condition (D0: black dots, AP_Ctrl: gray triangles, AP_BAC: pink squares, CP_Ctrl: blue crosses, CP_BAC: purple squares) on the same dimensions.

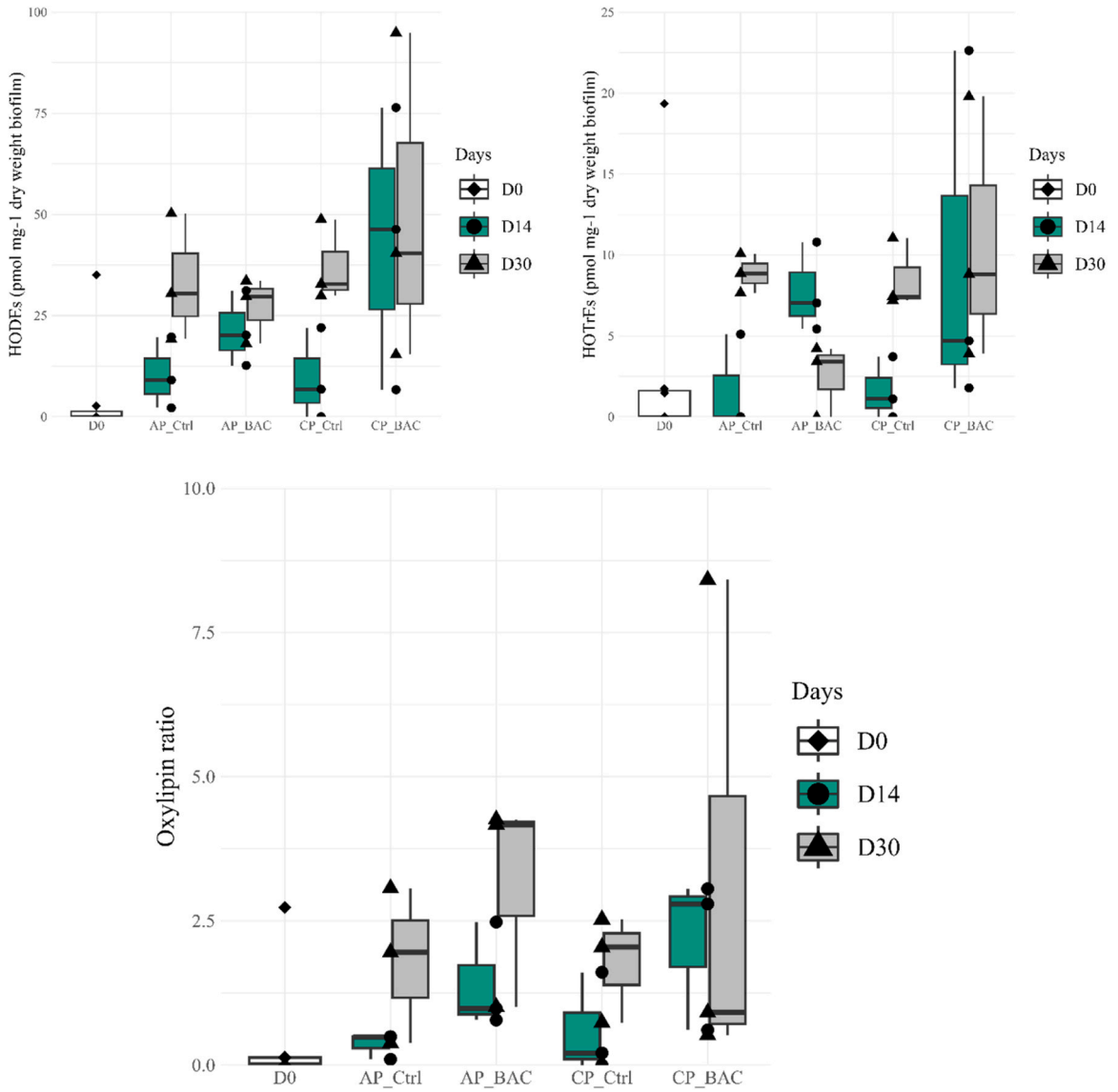

Fig. 6. Concentrations of HODEs and HOTrEs (in pmol mg^{-1} dry weight biofilm) and oxylipin ratio (in per thousand Eq. 2), as a function of the experimental conditions and exposure duration (Day 0-D0: diamonds, white; Day 14-D14: dots, green; Day 30-D30: triangles, gray). AP: Alternate photoperiod, CP: Continuous photoperiod, with DDBAC when indicated.

or Wang and Jia [88]. The latter results showed a decrease in populations of photoautotrophs (diatoms, cyanobacteria; [32]), and a decrease in chlorophyll *a* concentration [88] under continuous light exposure. In our study, changes in algal composition were also observed under CP conditions, with a decrease in green algae in the favour of diatoms but no effect on cyanobacteria. With fatty acids, such taxonomic shifts were highlighted by a change of membrane lipids composition (Fig. 4) from abundant C16:3, C16:4, C18:3 and C18:4 (markers of green algae; [24]) to increased C20:5 (marker of diatoms; [8]). However, a reduction of C16:3, C16:4, C18:3 and C18:4 was also highlighted in storage lipids but not accompanied by an increase of C20:5 (Fig. 5), suggesting that the light-induced stress was sufficient to change the composition of membrane but not enough that of storage lipids.

Apart from the aforementioned effects on biofilm taxonomic composition and specific lipid markers seen on the ACP, lipids and fatty acid composition did not show changes as striking related to ALAN conditions as observed by e.g., Napolitano [64]. Light intensity can affect the lipid composition of various organisms like diatoms [10] and green algae [64]. For example, Brown et al. [10] observed that microalgae were poorer in saturated fatty acids and monosaturated fatty acids after 10 days of exposure to ALAN at 50 µmol m^{-2} s^{-1} than microalgae exposed at 100 µmol m^{-2} s^{-1}. The incident light that Brown et al. [10] used in their experiment is close to our experimental conditions (91 ± 39 µmol m^{-2} s^{-1} at the surface of the beakers). Napolitano [64] also showed that green algae presented less polar lipids and more TAGs after a 7-day exposure to high light intensity as compared to lower intensity during the same period. In our study, such differences between FA groups and concentrations in membrane lipids were not highlighted. However, the aforementioned studies dealing with ALAN effects on lipids or fatty acids mainly relied on algal monocultures (*Thalassiosira pseudonana*, [10]; *Cladophora spp.*, [64]; *Chlorella vulgaris*, [2]) rather than on whole biofim communities.

4.2. DDBAC impacts on biofilms

DDBAC concentrations in the water of the contaminated conditions did not match the nominal concentration of 100 µg L^{-1}, even in the abiotic condition. This is likely to be the consequence of partial sorption of the contaminant on the experimental system, a common drawback in toxicological chemistry [13,91]. Biofilms in the contaminated condition were

exposed to low doses (compared to the environmental concentrations reported in Antunes et al. [3], with observed DDBAC concentrations in the experimental system averaging 1.2 ± 0.3 μg L^{-1}). The decrease in dissolved DDBAC was almost immediate in the systems containing biofilms, while it occurred at a longer term under abiotic conditions. Similarly, Chen et al. [13] reported a 30 % difference between expected and actual DDBAC concentrations, and explained this discrepancy by a sorption to the glass beaker. Concomitantly, DDBAC was quantified in the biofilms at concentrations of 0.980 ± 0.632 ng mg^{-1} dry weight (average concentrations for D14-D30), suggesting at least partial removal by the biological matrix. Indeed, the n-octanol-water partition coefficient (log K_{ow}) of DDBAC (2.93, [1]) suggests affinity of the compound with biological material, which is confirmed by its binding potential with organic matter (log Kd = 3, [22]). QACs can be adsorbed by a wide variety of organic materials such as sewage sludge [14], sediments [85,96], bacterial cell walls, clay, and humic materials [85]. The sorption of QACs depends on the length of carbon chains, the longer the carbon chain, the higher the sorption. In the biotic conditions, the decrease in DDBAC was likely due to simultaneous sorption on abiotic and biotic surfaces (including EPS) and possible biodegradation. Using another organic compound, the herbicide diuron, Chaumet et al. [11] also demonstrated rapid bioaccumulation by biofilm organisms and within EPS, concomitant to a decrease in dissolved diuron concentrations in the water. Here, DDBAC bioaccumulation reached a value of log(BCF)= 2.97 ± 0.16, which falls in the range of values obtained for the same compound in an experiment performed on biofilms for a shorter duration (10 days) and with a concentration 300 times higher than in this study (nominal concentration: 30 mg L^{-1}, [87]). DDBAC accumulation in biofilms may have occurred within living cells as well as in the EPS, although our analysis protocol did not allow to distinguish between biofilm fractions. Increased production of EPS in the presence of BAC was shown by Nakamura et al. [63], and interpreted as a protective mechanism. Li et al. [46] exposed the green alga *Chlorella vulgaris* to another QAC, cetyltrimethyl trimethyl ammonium chloride (CTAC) in the presence and absence of EPS; they showed an interaction between EPS and CTAC exposure, highlighted by the presence of EPS, the CTAC-induced stress decrease on the algae.

Contrary to Vrba et al. [87] and Ge et al. [29], our study did not show any decrease in photosynthetic efficiency in presence of DDBAC. Ge et al. [29] exposed microalgae for 10 days to several concentrations of DDBAC ranging from 3 to 48 mg L^{-1}, and found that photosynthesis was impacted from the lowest concentration tested. Vrba et al. [87] also found a striking decrease of PSII yields in biofilms exposed to 30 mg L^{-1} of DDBAC, from the second day of exposure in artificial channels, remaining visible until 10 days of experiment. However, in the present study, we used much lower concentrations than the above-mentioned studies, so that the photosynthetic efficiency of biofilms was not specifically impacted by DDBAC on the dates of sampling (after 14 and 30 days of exposure). The most striking effects of DDBAC were found herein in the fatty acid composition of membrane and storage lipids (Figs. 4 and 5) and oxylipins. A decrease in essential polyunsaturated fatty acids, such as some omega-3 and omega-6, could alter the nutritional quality of biofilms, and therefore decrease the energy supply along the food chain, with consequences on the entire ecosystem [9]. Mazzella et al. [52] also showed a decrease of PUFAs in biofilms with DDBAC. In this study, at D0, the biofilms contained higher amounts of C20:3 (likely an omega-6 FA) and PUFAs compared to D30 exposed to DDBAC in membrane lipids. Such a decrease in PUFAs in the favor of high amounts of SFA (saturated fatty acids) like C12:0, C14:0 and C16:0 on D30, suggests a decrease in the nutritional quality of biofilms for the food chain, as omega-3 and omega-6 are essential FA for energy transfer through trophic interactions [82]. In storage lipids, at D0, omega-6 FAs (like C18:3, C22:5) and PUFAs were largely abundant in biofilms, but only C16:0 and C16:1 remained at D30. Therefore, DDBAC possibly impacts aquatic food-chains through impairment of the transfer efficiency of these FAs from microalgae to consumers.

DDBAC is able to penetrate the cell and thus modifies cellular integrity [34,47,72]. Liu et al. [47] showed a link between the membrane integrity and the quantities of lipopolysaccharides (LPS). In fact, in bacteria exposed to DDBAC, LPS quantities decreased, and the expression of lipoprotein-related genes was upregulated, increasing membrane permeability. Han et al. [34] showed that QACs enhanced membrane permeability in bacterial cells and the production of ROS, potentially increasing oxylipin production. DDBAC exposure can also induce ROS production, as shown in the cyanobacteria *Microcystis aeruginosa* [95]. Entry of DDBAC into the cell likely resulted in the increase in oxylipin observed in our study, as shown by concentrations of HODEs and HOTrEs. These oxylipins derive from the respective degradation of C18:2 and C18:3 PUFAs, which could be caused by an oxydative stress [69]. These fatty acids are biomarkers of green algae and cyanobacteria [44,68]. Contrastingly, HEPEs originating from C20:5 were not found here. In Fig. 4, C20:5 was present in all conditions on D30 (with values ranging between 17 to 8%). It can be argued that DDBAC has a toxic effect on the PUFA of green algae but do not affect diatoms. Changes in oxylipin profiles were documented for several aquatic organisms. A specific increase in oxylipins following exposure to nitric oxide were already described on microorganisms by Johnson et al. [41], using the diatom *Phaeodactylum tricornutum* as a model species. Other studies on macroalgae facing heavy metal stress showed an increase in oxylipins [86]. Similar responses were also found with macrofauna: exposure of *Daphnia magna* to psychiatric drugs impacted their oxylipin profiles [27]. In addition, studies considering oxylipins along trophic chains have shown that feeding copepods with food containing oxylipins can cause infertility to the consumers [25,57,70]. Therefore, oxylipin production by biofilms exposed to DDBAC also possibly impairs other components of aquatic communities functioning. As such, oxylipins appear as good biomarkers of oxidative stress in natural environments [26,74]. In our study, oxylipins revealed to be relevant biomarkers for benthic microalgae in response to a toxic exposure; they are sensitive and relevant for detecting oxidative stress, in the face of an emerging chemical pollutant.

4.3. Combined effects of ALAN and DDBAC on biofilms

In natural conditions, more than two simultaneous stresses can impact the structure and functioning of biofilms, especially in urban areas. Unfortunately, our experimental design (three independent replicates) did not allow for a robust statistical assessment of the interactive effects of time, DDBAC and ALAN on the biofilms. As stated above, we demonstrated effects specific of each stressor; DDBAC increased oxylipin production, while ALAN impacted biofilm photosynthesis. However, under combined stressors, several descriptors exhibited more heterogenous responses than with exposure to a single stressor. Indeed, inter-replicate variability was much higher for total chlorophyll on day 14 (Fig. 2), for MUFA and PUFA proportions in storage lipids, as well as in oxylipins (HODEs, HOTrEs and oxylipin ratio) on both day 14 and day 30 (Fig. 6). To fully comprehend the possible interaction between ALAN and DDBAC on biofilms, additional data or research are crucially needed. Deleterious impacts on this basal resource of aquatic ecosystems can indeed have cascading effects on higher trophic components, and finally on human health. Therefore, more studies are required to describe the effects of urban stressors, alone and combined.

5. Conclusions

This study highlights the impacts of two urban pollutants of different nature (physical, chemical) on aquatic biofilms. We found that toxicants shared the same cellular targets as excess light, with the generation of ROS likely to damage the photosynthetic systems in microalgae. In contrast to our expectations though, the effects on biofilms were quite specific of the type of stress. Indeed, ALAN caused changes in the

microalgal composition and altered the photosynthetic function of the biofilm (photosynthetic yield). DDBAC seemed to modify lipid profiles in biofilms and to provoke specific oxidative stress on fatty acids, as highlighted by the presence of HODE and HOTrE oxylipins. Our results could not readily address the interaction between both stressors on the descriptors studied. However, laboratory conditions in this work were simplified as compared to the diversity of potential urban stressors faced simultaneously by the biota in natural environments. We recommend to investigate the long term impact of urban stressors *in situ* on biofilm fatty acid composition with a focus on oxylipins, to confirm the potential of this biomarker as an indicator of ecosystem impairment.

Environmental implications

Our study addressed the effects of two anthropogenic threats to aquatic biodiversity in urban environments: biocide contamination (DDBAC) and artificial light at night (ALAN). ALAN is ubiquitous, affecting all aquatic environments worldwide, while DDBAC is increasingly present in urban environments. We demonstrated that ALAN affects the photosynthesis of microalgal communities and that DDBAC exposure increases oxylipin production by the biofilms, which represent basal resources of most aquatic food chains in urban environments and elsewhere. This work confirms that stressors typical of urban environments deserve more research, in particular under more realistic (natural) conditions and taking into account possible interactive effects.

CRediT authorship contribution statement

Cassandre Madru: Methodology, Investigation, Conceptualization. **Débora Millan-Navarro**: Investigation. **Gwilherm Jan**: Resources. **Nicolas Mazzella**: Writing – review & editing, Resources, Methodology, Investigation. **Aurélie Moreira**: Writing – review & editing, Investigation. **Jacky Vedrenne**: Writing – review & editing, Resources. **Laure Carassou**: Writing – review & editing, Project administration, Methodology, Funding acquisition, Formal analysis, Conceptualization. **Soizic Morin**: Writing – review & editing, Writing – original draft, Supervision, Project administration, Methodology, Investigation, Conceptualization. **Caroline Roux**: Writing – review & editing, Writing – original draft, Project administration, Methodology, Investigation, Formal analysis, Conceptualization.

Funding

This work was supported by the Aqua department of INRAE and the Nature Division of Bordeaux Métropole as part of the shared research and development agreement relating to the Biodiver'Cité action plan (including grants from Bordeaux Métropole, Agence de l'Eau Adour Garonne, Département de la Gironde, and Région Nouvelle-Aquitaine).

Declaration of Competing Interest

The authors declare that they have no known competing financial interests or personal relationships that could have appeared to influence the work reported in this paper.

Data availability

Data will be made available on request.

Acknowledgements

The authors would like to thank Maud PIERRE for discussions on the statistical tests to be chosen, Margaux HERSCHEL for advices on the Graphical Abstract, and A.M. Lassallette for her help in editing the English style and grammar.

This work was carried out with the support (equipment and staff) provided by the XPO scientific infrastructure (DOI: 10.17180/breymr38; part of LIFE -Living in Freshwater and Estuaries- research infrastructure, INRAE) of EABX research unit. This work was also supported by the Bordeaux Metabolome Facility, the MetaboHUB (ANR11-INBS-0010) and the PHENOME (ANR-11-INBS-0012) projects.

Appendix A. Supporting information

Supplementary data associated with this article can be found in the online version at doi:10.1016/j.jhazmat.2024.134523.

References

[1] Abbott, T., Kor-Bicakci, G., Islam, M.S., Eskicioglu, C., 2020. A review on the fate of legacy and alternative antimicrobials and their metabolites during wastewater and sludge treatment. Article 23. Int J Mol Sci 21 (23) https://doi.org/10.3390/ijms21239241.

[2] Amini Khoeyi, Z., Seyfabadi, J., Ramezanpour, Z., 2012. Effect of light intensity and photoperiod on biomass and fatty acid composition of the microalgae, Chlorella vulgaris. Aquac Int 20 (1), 41–49. https://doi.org/10.1007/s10499-011-9440-1.

[3] Antunes, S., Nunes, B., Rodrigues, S., Nunes, R., Fernandes, J.O., Correia, A.T., 2016. Effects of chronic exposure to benzalkonium chloride in Oncorhynchus mykiss: cholinergic neurotoxicity, oxidative stress, peroxidative damage and genotoxicity. Environ Toxicol Pharmacol 45, 115–122. https://doi.org/10.1016/j.etap.2016.04.016.

[4] Asada, K., 2006. Production and scavenging of reactive oxygen species in chloroplasts and their functions. Plant Physiol 141 (2), 391–396. https://doi.org/10.1104/pp.106.082040.

[5] Authority EFSA, E. F. S., 2013. Evaluation of monitoring data on residues of didecyldimethylammonium chloride (DDAC) and benzalkonium chloride (BAC). EFSA Support Publ 10 (9), 483E. https://doi.org/10.2903/sp.efsa.2013.EN-483.

[6] Barber, O.W., Hartmann, E.M., 2022. Benzalkonium chloride: a systematic review of its environmental entry through wastewater treatment, potential impact, and mitigation strategies. Crit Rev Environ Sci Technol 52 (15), 2691–2719. https://doi.org/10.1080/10643389.2021.1889284.

[7] Bennie, J., Davies, T.W., Cruse, D., Gaston, K.J., 2016. Ecological effects of artificial light at night on wild plants. J Ecol 104 (3), 611–620. https://doi.org/10.1111/1365-2745.12551.

[8] Berge, J.-P., Gouygou, J.-P., Dubacq, J.-P., Durand, P., 1995. Reassessment of lipid composition of the diatom, Skeletonema costatum. Phytochemistry 39 (5), 1017–1021. https://doi.org/10.1016/0031-9422(94)00156-N.

[9] Brett, M., Müller-Navarra, D., 1997. The role of highly unsaturated fatty acids in aquatic foodweb processes. Freshw Biol 38 (3), 483–499. https://doi.org/10.1046/j.1365-2427.1997.00220.x.

[10] Brown, M.R., Dunstan, G.A., Norwood, Suzanne J., Miller, K.A., 1996. Effects of harvest stage and light on the biochemical composition of the diatom Thalassiosira pseudonana1. J Phycol 32 (1), 64–73. https://doi.org/10.1111/j.0022-3646.1996.00064.x.

[11] Chaumet, B., Morin, S., Hourtané, O., Artigas, J., Delest, B., Eon, M., et al., 2019. Flow conditions influence diuron toxicokinetics and toxicodynamics in freshwater biofilms. Sci Total Environ 652, 1242–1251. https://doi.org/10.1016/j.scitotenv.2018.10.265.

[12] Cheloni, G., Cosio, C., Slaveykova, V.I., 2014. Antagonistic and synergistic effects of light irradiation on the effects of copper on Chlamydomonas reinhardtii. Aquat Toxicol 155, 275–282. https://doi.org/10.1016/j.aquatox.2014.07.010.

[13] Chen, Y., Geurts, M., Sjollema, S.B., Kramer, N.I., Hermens, J.L.M., Droge, S.T.J., 2014. Acute toxicity of the cationic surfactant C12-benzalkonium in different bioassays: how test design affects bioavailability and effect concentrations. Environ Toxicol Chem 33 (3), 606–615. https://doi.org/10.1002/etc.2465.

[14] Clara, M., Scharf, S., Scheffknecht, C., Gans, O., 2007. Occurrence of selected surfactants in untreated and treated sewage. Water Res 41 (19), 4339–4348. https://doi.org/10.1016/j.watres.2007.06.027.

[15] Davey, M.E., O'toole, G.A., 2000. Microbial biofilms: from ecology to molecular genetics. Microbiol Mol Biol Rev: MMBR 64 (4), 847–867. https://doi.org/10.1128/MMBR.64.4.847-867.2000.

[16] Demailly, F., Elfeky, I., Malbezin, L., Le Guédard, M., Eon, M., Bessoule, J.-J., et al., 2019. Impact of diuron and S-metolachlor on the freshwater diatom Gomphonema gracile: complementarity between fatty acid profiles and different kinds of ecotoxicological impact-endpoints. Sci Total Environ 688, 960–969. https://doi.org/10.1016/j.scitotenv.2019.06.347.

[17] Deng, X.-Y., Li, D., Wang, L., Hu, X.-L., Cheng, J., Gao, K., 2017. Potential toxicity of ionic liquid ([C12mim]BF4) on the growth and biochemical characteristics of a marine diatom *Phaeodactylum tricornutum*. Sci Total Environ 586, 675–684. https://doi.org/10.1016/j.scitotenv.2017.02.043.

[18] Elersek, T., Ženko, M., Filipič, M., 2018. Ecotoxicity of disinfectant benzalkonium chloride and its mixture with antineoplastic drug 5-fluorouracil towards alga Pseudokirchneriella subcapitata. PeerJ 6, e4986. https://doi.org/10.7717/peerj.4986.

[19] Erickson, E., Wakao, S., Niyogi, K.K., 2015. Light stress and photoprotection in Chlamydomonas reinhardtii. Plant J 82 (3), 449–465. https://doi.org/10.1111/tpj.12825.

[20] EU Regulation 358/2014. (2014). *L_2014304DE.01004301.xml.* ⟨https://eur-lex.europa.eu/legal-content/DE/TXT/HTML/?uri=CELEX%3A32014R1119⟩.

[21] Falchi, F., Cinzano, P., Duriscoe, D., Kyba, C.C.M., Elvidge, C.D., Baugh, K., et al., 2016. The new world atlas of artificial night sky brightness. Sci Adv 2 (6), e1600377. https://doi.org/10.1126/sciadv.1600377.

[22] Ferrer, I., Furlong, E.T., 2002. Accelerated solvent extraction followed by on-line solid-phase extraction coupled to ion trap LC/MS/MS for analysis of benzalkonium chlorides in sediment samples. Anal Chem 74 (6), 1275–1280. https://doi.org/10.1021/ac010969l.

[23] Filimonova, V., Gonçalves, F., Marques, J.C., De Troch, M., Gonçalves, A.M.M., 2016. Biochemical and toxicological effects of organic (herbicide Primextra® Gold TZ) and inorganic (copper) compounds on zooplankton and phytoplankton species. Aquat Toxicol 177, 33–43. https://doi.org/10.1016/j.aquatox.2016.05.008.

[24] Fisher, N.S., Schwarzenbach, R.P., 1978. Fatty acid dynamics in Thalassiosira pseudonana (bacillariophyceae): implications for P hysiological ecology1,2,3. J Phycol 14 (2), 143–150. https://doi.org/10.1111/j.1529-8817.1978.tb02439.x.

[25] Fontana, A., d'Ippolito, G., Cutignano, A., Romano, G., Lamari, N., Massa Gallucci, A., et al., 2007. LOX-induced lipid peroxidation mechanism responsible for the detrimental effect of marine diatoms on zooplankton grazers. ChemBioChem 8 (15), 1810–1818. https://doi.org/10.1002/cbic.200700269.

[26] Galano, J.-M., Lee, Y.Y., Oger, C., Vigor, C., Vercauteren, J., Durand, T., et al., 2017. Isoprostanes, neuroprostanes and phytoprostanes: an overview of 25years of research in chemistry and biology. Prog Lipid Res 68, 83–108. https://doi.org/10.1016/j.plipres.2017.09.004.

[27] Garreta-Lara, E., Checa, A., Fuchs, D., Tauler, R., Lacorte, S., Wheelock, C.E., et al., 2018. Effect of psychiatric drugs on Daphnia magna oxylipin profiles. Sci Total Environ 644, 1101–1109. https://doi.org/10.1016/j.scitotenv.2018.06.333.

[28] Gaston, K.J., Duffy, J.P., Gaston, S., Bennie, J., Davies, T.W., 2014. Human alteration of natural light cycles: causes and ecological consequences. Oecologia 176 (4), 917–931. https://doi.org/10.1007/s00442-014-3088-2.

[29] Ge, Y., Chen, J., Xue, Y., Xing, W., Zhang, L., Lu, X., et al., 2024. Elimination of inhibitory effects of dodecyl dimethyl benzyl ammonium chloride on microalgae in wastewater by cocultivation with a newly screened microbial consortium. Sci Total Environ 919, 170676. https://doi.org/10.1016/j.scitotenv.2024.170676.

[30] Genty, B., Briantais, J.-M., Baker, N.R., 1989. The relationship between the quantum yield of photosynthetic electron transport and quenching of chlorophyll fluorescence. Biochim Et Biophys Acta (BBA) Gen Subj 990 (1), 87–92. https://doi.org/10.1016/S0304-4165(89)80016-9.

[31] Gerba, C.P., 2015. Quaternary ammonium biocides: efficacy in application. Appl Environ Microbiol 81 (2), 464–469. https://doi.org/10.1128/AEM.02633-14.

[32] Grubisic, M., Singer, G., Bruno, M.C., van Grunsven, R.H.A., Manfrin, A., Monaghan, M.T., et al., 2017. Artificial light at night decreases biomass and alters community composition of benthic primary producers in a sub-alpine stream: ALAN affects stream periphyton. Limnol Oceanogr 62 (6), 2799–2810. https://doi.org/10.1002/lno.10607.

[33] Hamilton, J.G., Comai, K., 1988. Separation of neutral lipid, free fatty acid and phospholipid classes by normal phase HPLC. Lipids 23 (12), 1150–1153. https://doi.org/10.1007/BF02535282.

[34] Han, Y., Zhou, Z.-C., Zhu, L., Wei, Y.-Y., Feng, W.-Q., Xu, L., et al., 2019. The impact and mechanism of quaternary ammonium compounds on the transmission of antibiotic resistance genes. Environ Sci Pollut Res 26 (27), 28352–28360. https://doi.org/10.1007/s11356-019-05673-2.

[35] Hill, G.T., Mitkowski, N.A., Aldrich-Wolfe, L., Emele, L.R., Jurkonie, D.D., Ficke, A., et al., 2000. Methods for assessing the composition and diversity of soil microbial communities. Appl Soil Ecol 15 (1), 25–36. https://doi.org/10.1016/S0929-1393(00)00069-X.

[36] Hölker, F., Wurzbacher, C., Weißenborn, C., Monaghan, M.T., Holzhauer, S.I.J., Premke, K., 2015. Microbial diversity and community respiration in freshwater sediments influenced by artificial light at night. Philos Trans R Soc B: Biol Sci 370 (1667), 20140130. https://doi.org/10.1098/rstb.2014.0130.

[37] Hu, Q., Sommerfeld, M., Jarvis, E., Ghirardi, M., Posewitz, M., Seibert, M., et al., 2008. Microalgal triacylglycerols as feedstocks for biofuel production: perspectives and advances. Plant J 54 (4), 621–639. https://doi.org/10.1111/j.1365-313X.2008.03492.x.

[38] Hua, X., Li, M., Su, Y., Dong, D., Guo, Z., Liang, D., 2012. The degradation of linear alkylbenzene sulfonate (LAS) in the presence of light and natural biofilms: the important role of photosynthesis. J Hazard Mater 229–230, 450–454. https://doi.org/10.1016/j.jhazmat.2012.06.005.

[39] Huner, N.P.A., Öquist, G., Melis, A., 2003. Photostasis in plants, green algae and cyanobacteria: the role of light harvesting antenna complexes. In: Green, B.R., Parson, W.W. (Eds.), Light-Harvesting Antennas in Photosynthesis. Springer Netherlands, pp. 401–421. https://doi.org/10.1007/978-94-017-2087-8_14.

[40] Ikuma, K., Decho, A.W., Lau, B.L.T., 2015. When nanoparticles meet biofilms—Interactions guiding the environmental fate and accumulation of nanoparticles. Front Microbiol 6. ⟨https://www.frontiersin.org/articles/10.3389/fmicb.2015.00591⟩.

[41] Johnson, M.D., Edwards, B.R., Beaudoin, D.J., Van Mooy, B.A.S., Vardi, A., 2020. Nitric oxide mediates oxylipin production and grazing defense in diatoms. Environ Microbiol 22 (2), 629–645. https://doi.org/10.1111/1462-2920.14879.

[42] Kümmerer, K., Eitel, A., Braun, U., Hubner, P., Daschner, F., Mascart, G., et al., 1997. Analysis of benzalkonium chloride in the effluent from European hospitals by solid-phase extraction and high-performance liquid chromatography with post-column ion-pairing and fluorescence detection. J Chromatogr A 774 (1), 281–286. https://doi.org/10.1016/S0021-9673(97)00242-2.

[43] Kyba, C.C.M., Ruhtz, T., Fischer, J., Hölker, F., 2011. Cloud coverage acts as an amplifier for ecological light pollution in urban ecosystems. PLoS One 6 (3), e17307. https://doi.org/10.1371/journal.pone.0017307.

[44] Lang, I., Hodac, L., Friedl, T., Feussner, I., 2011. Fatty acid profiles and their distribution patterns in microalgae: a comprehensive analysis of more than 2000 strains from the SAG culture collection. BMC Plant Biol 11 (1), 124. https://doi.org/10.1186/1471-2229-11-124.

[45] Larsson, Y., Mongelli, A., Kisielius, V., Bester, K., 2024. Microbial biofilm metabolization of benzalkonium compounds (benzyl dimethyl dodecyl ammonium & benzyl dimethyl tetradecyl ammonium chloride). J Hazard Mater 463, 132834. https://doi.org/10.1016/j.jhazmat.2023.132834.

[46] Li, F., Kuang, Y., Liu, N., Ge, F., 2019. Extracellular polymeric substrates of Chlorella vulgaris F1068 weaken stress of cetyltrimethyl ammonium chloride on ammonium uptake. Sci Total Environ 661, 678–684. https://doi.org/10.1016/j.scitotenv.2018.12.472.

[47] Liu, C., Goh, S.G., You, L., Yuan, Q., Mohapatra, S., Gin, K.Y.-H., et al., 2023. Low concentration quaternary ammonium compounds promoted antibiotic resistance gene transfer via plasmid conjugation. Sci Total Environ 887, 163781. https://doi.org/10.1016/j.scitotenv.2023.163781.

[48] MacIntyre, H.L., Kana, T.M., Anning, T., Geider, R.J., 2002. Photoacclimation of photosynthesis irradiance response curves and photosynthetic pigments in microalgae and cyanobacteria1. J Phycol 38 (1), 17–38. https://doi.org/10.1046/j.1529-8817.2002.00094.x.

[49] Maggi, E., Bertocci, I., Benedetti-Cecchi, L., 2020. Light pollution enhances temporal variability of photosynthetic activity in mature and developing biofilm. Hydrobiologia 847 (7), 1793–1802. https://doi.org/10.1007/s10750-019-04102-2.

[50] Maggi, E., Bongiorni, L., Fontanini, D., Capocchi, A., Dal Bello, M., Giacomelli, A., et al., 2019. Artificial light at night erases positive interactions across trophic levels. Funct Ecol 34 (3), 694–706. https://doi.org/10.1111/1365-2435.13485.

[51] Martínez-Carballo, E., Sitka, A., González-Barreiro, C., Kreuzinger, N., Fürhacker, M., Scharf, S., et al., 2007. Determination of selected quaternary ammonium compounds by liquid chromatography with mass spectrometry. Part I. Application to surface, waste and indirect discharge water samples in Austria. Environ Pollut 145 (2), 489–496. https://doi.org/10.1016/j.envpol.2006.04.033.

[52] Mazzella, N., Moreira, A., Eon, M., Médina, A., Millan-Navarro, D., Creusot, N., 2023. Hydrophilic interaction liquid chromatography coupled with tandem mass spectrometry method for quantification of five phospholipid classes in various matrices. MethodsX 10, 102026. https://doi.org/10.1016/j.mex.2023.102026.

[53] Mazzella, N., Vrba, R., Moreira, A., Creusot, N., Eon, M., MillanNavarro, D., et al., 2023. Mixed light photoperiod and biocide pollution affect lipid profiles of periphyton communities in freshwater ecosystems. J Hazard Mater Adv 12, 100378. https://doi.org/10.1016/j.hazadv.2023.100378.

[54] McElhaney, R.N., De Gier, J., Van Der Neut-Kok, E.C.M., 1973. The effect of alterations in fatty acid composition and cholesterol content on the nonelectrolyte permeability of Acholeplasma laidlawii B cells and derived liposomes. Biochim Et Biophys Acta (BBA) - Biomembr 298 (2), 500–512. https://doi.org/10.1016/0005-2736(73)90376-3.

[55] McNamara, P.J., Levy, S.B., 2016. Triclosan: an instructive tale. Antimicrob Agents Chemother 60 (12), 7015–7016. https://doi.org/10.1128/aac.02105-16.

[56] Merchel Piovesan Pereira, B., Tagkopoulos, I., 2019. Benzalkonium chlorides: uses, regulatory status, and microbial resistance. Appl Environ Microbiol 85 (13), e00377–19. https://doi.org/10.1128/AEM.00377-19.

[57] Miralto, A., Barone, G., Romano, G., Poulet, S.A., Ianora, A., Russo, G.L., et al., 1999. The insidious effect of diatoms on copepod reproduction. Article 6758. Nature 402 (6758) https://doi.org/10.1038/46023.

[58] Mohapatra, S., Bhatia, S., Senaratna, K.Y.K., Jong, M.-C., Lim, C.M.B., Gangesh, G. R., et al., 2023. Wastewater surveillance of SARS-CoV-2 and chemical markers in campus dormitories in an evolving COVID − 19 pandemic. J Hazard Mater 446, 130690. https://doi.org/10.1016/j.jhazmat.2022.130690.

[59] Moore, L.E., Ledder, R.G., Gilbert, P., Mcbain, A.J., 2008. In vitro study of the effect of cationic biocides on bacterial population dynamics and susceptibility. Appl Environ Microbiol 74 (15), 4825–4834. https://doi.org/10.1128/AEM.00573-08.

[60] Moore, M.V., Pierce, S.M., Walsh, H.M., Kvalvik, S.K., Lim, J.D., 2000. Urban light pollution alters the diel vertical migration of Daphnia. Int Ver Für Theor Und Angew Limnol: Verh 27 (2), 779–782. https://doi.org/10.1080/03680770.1998.11901341.

[61] Mora, J., Freixa, A., Perujo, N., & Barral-Fraga, L. (2016). *Limits of the Biofilm Concept and Types of Aquatic Biofilms* (p. 24). ⟨https://doi.org/10.21775/9781910190173.01⟩.

[62] Mulder, I., Siemens, J., Sentek, V., Amelung, W., Smalla, K., Jechalke, S., 2018. Quaternary ammonium compounds in soil: implications for antibiotic resistance development. Rev Environ Sci Bio/Technol 17 (1), 159–185. https://doi.org/10.1007/s11157-017-9457-7.

[63] Nakamura, H., Takakura, K.-I., Sone, Y., Itano, Y., Nishikawa, Y., 2013. Biofilm formation and resistance to benzalkonium chloride in *Listeria monocytogenes* isolated from a fish processing plant. J Food Prot 76 (7), 1179–1186. https://doi.org/10.4315/0362-028X.JFP-12-225.

[64] Napolitano, G.E., 1994. The relationship of lipids with light and chlorophyll measurements in freshwater algae and periphyton1. J Phycol 30 (6), 943–950. https://doi.org/10.1111/j.0022-3646.1994.00943.x.

[65] Pajot, A., Lavaud, J., Carrier, G., Lacour, T., Marchal, L., Nicolau, E., 2023. Light-response in two clonal strains of the haptophyte Tisochrysis lutea: Evidence for

different photoprotection strategies. Algal Res 69, 102915. https://doi.org/10.1016/j.algal.2022.102915.
[66] Pethybridge, H.R., Parrish, C.C., Morrongiello, J., Young, J.W., Farley, J.H., Gunasekera, R.M., et al., 2015. Spatial patterns and temperature predictions of tuna fatty acids: tracing essential nutrients and changes in primary producers. PLoS ONE 10 (7), e0131598. https://doi.org/10.1371/journal.pone.0131598.
[67] Poulin, C., Bruyant, F., Laprise, M.-H., Cockshutt, A.M., Marie-Rose Vandenhecke, J., Huot, Y., 2014. The impact of light pollution on diel changes in the photophysiology of Microcystis aeruginosa. J Plankton Res 36 (1), 286–291. https://doi.org/10.1093/plankt/fbt088.
[68] Renaud, S.M., Thinh, L.-V., Parry, D.L., 1999. The gross chemical composition and fatty acid composition of 18 species of tropical Australian microalgae for possible use in mariculture. Aquaculture 170 (2), 147–159. https://doi.org/10.1016/S0044-8486(98)00399-8.
[69] Ritter, A., Goulitquer, S., Salaün, J.-P., Tonon, T., Correa, J.A., Potin, P., 2008. Copper stress induces biosynthesis of octadecanoid and eicosanoid oxygenated derivatives in the brown algal kelp Laminaria digitata. N Phytol 180 (4), 809–821. https://doi.org/10.1111/j.1469-8137.2008.02626.x.
[70] Ruocco, N., Albarano, L., Esposito, R., Zupo, V., Costantini, M., Ianora, A., 2020. Multiple roles of diatom-derived oxylipins within marine environments and their potential biotechnological applications. Mar Drugs 18 (7), 342. https://doi.org/10.3390/md18070342.
[71] Serôdio, J., Ezequiel, J., Barnett, A., Mouget, J.-L., Méléder, V., Laviale, M., et al., 2012. Efficiency of photoprotection in microphytobenthos: role of vertical migration and the xanthophyll cycle against photoinhibition. Aquat Microb Ecol 67, 161. https://doi.org/10.3354/ame01591.
[72] Severina, I.I., Muntyan, M.S., Lewis, K., Skulachev, V.P., 2001. Transfer of cationic antibacterial agents berberine, palmatine, and benzalkonium through bimolecular planar phospholipid film and staphylococcus aureus membrane. IUBMB Life 52 (6), 321–324. https://doi.org/10.1080/152165401317291183.
[73] Smyth, T.J., Wright, A.E., McKee, D., Tidau, S., Tamir, R., Dubinsky, Z., et al., 2021. A global atlas of artificial light at night under the sea. Elem: Sci Anthr 9 (1), 00049. https://doi.org/10.1525/elementa.2021.00049.
[74] Späth, J., Brodin, T., Cerveny, D., Lindberg, R., Fick, J., Nording, M.L., 2021. Oxylipins at intermediate larval stages of damselfly Coenagrion hastulatum as biochemical biomarkers for anthropogenic pollution. Environ Sci Pollut Res Int 28 (22), 27629–27638. https://doi.org/10.1007/s11356-021-12503-x.
[75] Spitschan, M., Aguirre, G.K., Brainard, D.H., Sweeney, A.M., 2016. Variation of outdoor illumination as a function of solar elevation and light pollution. Article 1 Sci Rep 6 (1). https://doi.org/10.1038/srep26756.
[76] Sreevidya, V.S., Lenz, K.A., Svoboda, K.R., Ma, H., 2018. Benzalkonium chloride, benzethonium chloride, and chloroxylenol—three replacement antimicrobials are more toxic than triclosan and triclocarban in two model organisms. Environ Pollut 235, 814–824. https://doi.org/10.1016/j.envpol.2017.12.108.
[77] Stevens, R.G., Zhu, Y., 2015. Electric light, particularly at night, disrupts human circadian rhythmicity: is that a problem. Philos Trans R Soc B: Biol Sci 370 (1667), 20140120. https://doi.org/10.1098/rstb.2014.0120.
[78] Strandberg, U., Hiltunen, M., Jelkänen, E., Taipale, S.J., Kainz, M.J., Brett, M.T., et al., 2015. Selective transfer of polyunsaturated fatty acids from phytoplankton to planktivorous fish in large boreal lakes. Sci Total Environ 536, 858–865. https://doi.org/10.1016/j.scitotenv.2015.07.010.
[79] Strassburg, K., Huijbrechts, A.M.L., Kortekaas, K.A., Lindeman, J.H., Pedersen, T. L., Dane, A., et al., 2012. Quantitative profiling of oxylipins through comprehensive LC-MS/MS analysis: application in cardiac surgery. Anal Bioanal Chem 404 (5), 1413–1426. https://doi.org/10.1007/s00216-012-6226-x.
[80] Sukenik, A., Bennett, J., Falkowski, P., 1987. Light-saturated photosynthesis—limitation by electron transport or carbon fixation? Biochim Et Biophys Acta (BBA) - Bioenerg 891 (3), 205–215. https://doi.org/10.1016/0005-2728(87)90216-7.
[81] Sutherland, I.W., 2001. The biofilm matrix – an immobilized but dynamic microbial environment. Trends Microbiol 9 (5), 222–227. https://doi.org/10.1016/S0966-842X(01)02012-1.
[82] Taipale, S., Strandberg, U., Peltomaa, E., Galloway, A.W.E., Ojala, A., Brett, M.T., 2013. Fatty acid composition as biomarkers of freshwater microalgae: analysis of 37 strains of microalgae in 22 genera and in seven classes. Aquat Microb Ecol 71 (2), 165–178. https://doi.org/10.3354/ame01671.
[83] Twining, C.W., Bernhardt, J.R., Derry, A.M., Hudson, C.M., Ishikawa, A., Kabeya, N., et al., 2021. The evolutionary ecology of fatty-acid variation: implications for consumer adaptation and diversification. Ecol Lett 24 (8), 1709–1731. https://doi.org/10.1111/ele.13771.
[84] US EPA, O. (2020, April 14). *Disinfectant Use and Coronavirus (COVID-19)* [Overviews and Factsheets]. ⟨https://www.epa.gov/coronavirus/disinfectant-use-and-coronavirus-covid-19⟩.
[85] van Wijk, D., Gyimesi-van den Bos, M., Garttener-Arends, I., Geurts, M., Kamstra, J., Thomas, P., 2009. Bioavailability and detoxification of cationics: I. Algal toxicity of alkyltrimethyl ammonium salts in the presence of suspended sediment and humic acid. Chemosphere 75 (3), 303–309. https://doi.org/10.1016/j.chemosphere.2008.12.047.
[86] Vigor, C., Reversat, G., Rocher, A., Oger, C., Galano, J.-M., Vercauteren, J., et al., 2018. Isoprostanoids quantitative profiling of marine red and brown macroalgae. Food Chem 268, 452–462. https://doi.org/10.1016/j.foodchem.2018.06.111.
[87] Vrba, R. , Lavoie, I. , Creusot, N. , Eon, M. , Millan-Navarro, D. , Feurtet-Mazel, A. et al. (2023). Experimental testing of two urban stressors on freshwater biofilms (p. 2023.06.11.544504). bioRxiv. ⟨https://doi.org/10.1101/2023.06.11.544504⟩.
[88] Wang, B., Jia, J., 2020. Photoprotection mechanisms of Nannochloropsis oceanica in response to light stress. Algal Res 46, 101784. https://doi.org/10.1016/j.algal.2019.101784.
[89] Wang, G., Yang, L., Jiang, L., Chen, J., Jing, Q., Mai, Y., et al., 2022. A new class of quaternary ammonium compounds as potent and environmental friendly disinfectants. J Clean Prod 379, 134632. https://doi.org/10.1016/j.jclepro.2022.134632.
[90] Waring, J., Klenell, M., Bechtold, U., Underwood, G.J.C., Baker, N.R., 2010. Light-induced responses of oxygen photoreduction, reactive oxygen species production and scavenging in two diatom species1. J Phycol 46 (6), 1206–1217. https://doi.org/10.1111/j.1529-8817.2010.00919.x.
[91] Wilms, W., Woźniak-Karczewska, M., Niemczak, M., Lisiecki, P., Zgoła-Grześkowiak, A., Ławniczak, Ł., et al., 2020. Quantifying the mineralization of 13C-labeled cations and anions reveals differences in microbial biodegradation of herbicidal ionic liquids between water and soil. ACS Sustain Chem Eng 8 (8), 3412–3426. https://doi.org/10.1021/acssuschemeng.9b07598.
[92] Yang, K., Chen, M.-L., Zhu, D., 2023. Exposure to benzalkonium chloride disinfectants promotes antibiotic resistance in sewage sludge microbiomes. Sci Total Environ 867, 161527. https://doi.org/10.1016/j.scitotenv.2023.161527.
[93] Yang, Z., Geng, L., Wang, W., Zhang, J., 2012. Combined effects of temperature, light intensity, and nitrogen concentration on the growth and polysaccharide content of Microcystis aeruginosa in batch culture. Biochem Syst Ecol 41, 130–135. https://doi.org/10.1016/j.bse.2011.12.015.
[94] Zelles, L., 1999. Fatty acid patterns of phospholipids and lipopolysaccharides in the characterisation of microbial communities in soil: a review. Biol Fertil Soils 29 (2), 111–129. https://doi.org/10.1007/s003740050533.
[95] Zhang, C., Zhang, X., Chen, Q., Ye, S., Li, B., Pan, B., et al., 2024. Variations in growth, photosynthesis, oxidative stress and microcystin production in *Microcystis aeruginosa* caused by acute exposure to Benzalkonium Chloride and Benzalkonium Bromide. Process Saf Environ Prot 182, 1110–1120. https://doi.org/10.1016/j.psep.2023.12.058.
[96] Zhang, C., Cui, F., Zeng, G., Jiang, M., Yang, Z., Yu, Z., et al., 2015. Quaternary ammonium compounds (QACs): a review on occurrence, fate and toxicity in the environment. Sci Total Environ 518–519, 352–362. https://doi.org/10.1016/j.scitotenv.2015.03.007.
[97] Zheng, G., Webster, T.F., Salamova, A., 2021. Quaternary ammonium compounds: bioaccumulation potentials in humans and levels in blood before and during the Covid-19 pandemic. Environ Sci Technol 55 (21), 14689–14698. https://doi.org/10.1021/acs.est.1c01654.
[98] Zhu, X., Wang, Z., Sun, Y., Gu, L., Zhang, L., Wang, J., et al., 2020. Surfactants at environmentally relevant concentrations interfere the inducible defense of Scenedesmus obliquus and the implications for ecological risk assessment. Environ Pollut 261, 114131. https://doi.org/10.1016/j.envpol.2020.114131.
[99] Zissis, G., & Bertoldi, P. (2018). *Status of LED-Lighting world market in 2017* [Ispra]. European Commission.